

Adaptive Optics - Principles and Application

SeBeom Lee

Astro 301

2017 May 05

ABSTRACT

Adaptive optics is a technology of reconstructing images that are distorted by a turbulence in Earth's atmosphere. The process of adaptive optics can be divided into three parts: distortion by the atmosphere, wavefront sensor, and the deformable mirror. In this paper, we analysed the modeling of the atmosphere based on the Kolmogorov turbulence model, investigated the wavefront sensor using a Shack-Hartmann sensor, and explored various types of deformable mirrors and techniques used to deform mirrors. Based on the analysis of three steps of the technology, I created a simulation that duplicates the process of adaptive optics and simulated a distortion of image by an atmosphere and the reconstruction of it by an adaptive process.

1. Introduction

1.1. What is adaptive optics?

Telescopes have played a vital role in the development of astronomy. After the invention of telescope by Hans Lippershey in 1608, the technology has enabled a lot of important discoveries. In the age of Galileo Galilei, most of the observers depended on telescopes, and Galilei himself made a lot of crucial discoveries using telescope, such as moon craters, sunspots, and moons of Jupiter. The situation is not very different nowadays. A lot of important observations such as redshift, which later helped scientists to investigate expansion of universe, and new planets, stars, and galaxies are based on telescope technology. Because of such an important place of telescope in the field of astronomy, achieving a high precision has always been a crucial task for scientists. A well-known method of increasing the accuracy of telescope image is to improve the angular resolution, which depends on the diameter of the collecting area. A rough estimate of the angular resolution can be

expressed by the Rayleigh criterion.

$$\theta_{min} = 1.22 \frac{\lambda}{D} \quad (1)$$

According to Rayleigh criterion, a angular resolution depends on the wavelength of the light and the size of the aperture. A higher precision of telescope can be achieved as the wavelength of the light is shorter, and as the size of the aperture is bigger. Therefore, scientists have designed telescopes with larger disk, a collecting area, or wider telescope array. Such efforts have been successful in increasing the resolution of telescope, but there was a clear limit on this method. The lower bound of the angular resolution was about 1 *arcsec*, because of the turbulence in Earth's atmosphere. Scientists needed a novel method that can overcome this limitation, and an adaptive optics, a very powerful and promising technique for high precision observation, has emerged (Jacque M. Beckers 1993).

Adaptive optics is a technology that removes the noise in the image caused by the atmosphere. When an image information passes through Earth's atmosphere, its perturbation introduces a wavefront distortion. Using a mirror whose surface can be controlled to be deformed, adaptive optics removes the distortion to get a clean image. Wavefront distortion is calculated to find an appropriate deformation of mirror surface, and a widely used method is using a laser guidance star. Adaptive optics is usually confused with a similar technology, active optics. While adaptive optics is a technology that reduces a distortion caused by atmosphere, active optics is used to control errors introduced by mechanical, optical, and thermal effects in the telescope itself. Since these factors have rather a long term influence, active optics are slower than adaptive optics, whose purpose is to deal with rapidly changing atmosphere. In general, astronomical adaptive optics operates in frequency of 10 to 1000 Hz, while active optics is in less than 1 Hz (Jacque M. Beckers 1993).

1.2. History of adaptive optics

The concept of using adaptive optics to compensate atmospheric effect was first brought up by Horace W. Babcock in 1953 (Babcock 1953). In his paper "The possibility of compensating astronomical seeing," which is known as the first paper on adaptive optics, he describes various applications of the technology on military, laser power, medical, and other fields (Jacque M. Beckers 1993). Babcock's paper was remarkable in that it was more than just a suggestion of the concept. He explained a way of measuring the wavefront distortion, and proposed a concept for the adaptive mirror.

After Babcock's suggestion in 1953, a development of adaptive optics was largely limited to research in the military. While the research for the military application of adaptive optics was well funded by the government, that for astronomical applications received only limited amount of money, thereby slowing down the implementation of Babcock's suggestion. In the mid-1970s, Buffington and collaborators made their first attempt to utilize adaptive optics in astronomical observation. They came up with a one dimensional, 6-element segmented mirror with piston control.

Later, J. W. Hardy made another attempt with two dimensional, 21 actuator continuous surface deformable mirror combined with a shearing interferometer wavefront sensor. The results were promising in that they demonstrated the concept and showed a possibility for further improvement, but at the same time, they proved that a complex adaptive optics system requires a very high costs, making it less accessible to astronomers. In addition, they showed that the technology is only efficient for bright stars, and the news made many astronomers less enthusiastic about the technology (Jacque M. Beckers 1993).

However, interest in adaptive optics has resurged recently. The government had kept the technology classified during the 1970s and 1980s, but by early 1990s, a lot of information about the adaptive optics program, such as primary documents from Air Force Research lab, was declassified. A lot of private organizations could get an access to the information, and company like Itek could make an amazing progress in the development of the technology (Robert W. Duffner 2009). Also, Scientists realized that many limitations disappeared at infrared wavelengths. In infrared, the complexity of the adaptive optics system could be lowered a lot, as the number of adaptive elements and required control frequency decreased. As IR panoramic detectors become more available, scientists regained their interest in adaptive optics. Also, an invention of bright laser guide stars also contributed. Guide stars are objects used to calculate the wavefront distortion. Scientists use non-stellar objects like Galilean satellites as natural guide stars, but laser guide stars, artificial laser beacons, are much more efficient and manageable.

2. Principles of adaptive optics

The process for adaptive optics can be largely divided into three parts: distortion by atmosphere, wavefront sensor, and deformable mirror. Figure 1 shows an overall process of adaptive optics.

At the Earth's atmosphere, the first step of adaptive optics takes place. An optical aberration by the perturbation, mostly caused by turbulence, of atmosphere introduces a wavefront distortion to the image signal. Then, the distorted signal goes to next essential part, the deformable mirror, whose purpose is to reduce the distortion of the wavefront. To adjust the surface deformation of the mirror, a loop of the wavefront sensor and the control system for the mirror is formed. Using the split screen, the system sends an image signal to the wavefront sensor, and based on the calculation, the sensor gives a feedback to the control system to correct the deformation of mirror (Merkle 1986). In this paper, each part of the system will be investigated.

2.1. Distortion by the atmosphere

Wavefront distortion is mostly caused by the difference of refractive index. A turbulence of air mixes different layers of atmosphere and creates various eddies in the atmosphere, thereby creating

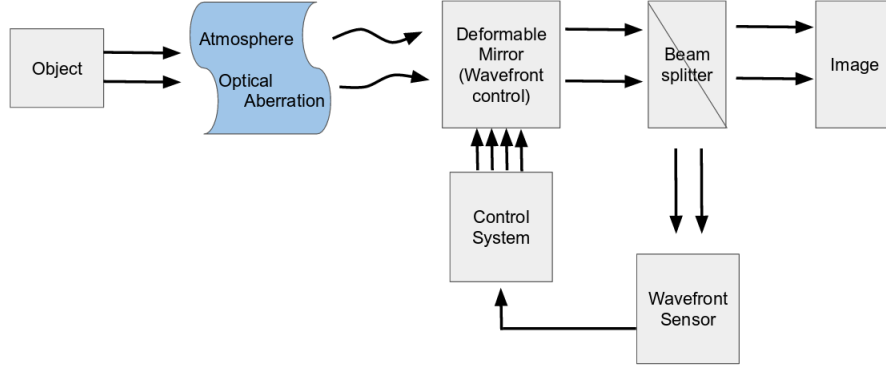


Fig. 1.— Principles of adaptive optics: An image signal from an object passes through the Earth’s atmosphere, and the wavefront is distorted by the perturbation in atmosphere. The wavefront distortion is removed by the deformable mirror, which is controlled by the loop connected to the wavefront sensor. By continuously correcting the mirror surface based on the result from wavefront sensor, the system compensates the influence of rapidly changing atmosphere.

different parts of atmosphere with different density and refractive index. Under the assumption that the turbulence is isotropic and homogeneous, the turbulence velocity field can be modeled by Kolmogorove structure function as follows (N. J. Woolf 1982).

$$D_v(R_1, R_2) = \left\langle |v(R_1) - v(R_2)|^2 \right\rangle \quad (2)$$

$$= \alpha f(|R_1 - R_2|/\beta) \quad (3)$$

By dimensional analysis, we can reach a conclusion that above equation can be expressed as follows, where C_v describes a turbulence strength.

$$D_v(R_1, R_2) = C_v^2 |R_1 - R_2|^{2/3} \quad (4)$$

Temperature fluctuation will follow a similar structure function with a new parameter C_T , and by the ideal gas law, we can derive that the refractive index also has a similar structure function.

$$D_n(R_1, R_2) = C_N^2 |R_1 - R_2|^{2/3} \quad (5)$$

Above equation implies that for different points of the atmosphere, the refractive indices will mostly differ by 2/3 power of the their horizontal displacement. Although the refractive index of atmosphere is near unity, as derived above, light rays passing through different parts of atmosphere will experience different refractive index, and as a result, wavefront will be distorted.

2.2. Wavefront sensor

To make deformable mirror to effectively reduce the noise, wavefront distortion introduced by the atmosphere must be known. A widely used method of wavefront measurement is a Shack-Hartmann test. The technique was first introduced by J. Hartmann (Hartmann 1900). The Hartmann test uses an array of charge-coupled devices (CCD), and detects the point the ray hits the sensor to calculate its diversion from the reference point. The technique was later improved by Roland Shack and Ben Platt by adding small spherical lenlets in front of the screen. By focusing rays on smaller region, they could achieve a higher efficiency, and as they could gather more points on smaller array, they could increase the filling factor of the sensor thereby enabling more sampling. Figure 2 shows a basic principle of the Shack-Hartmann sensor. The lens focuses incoming wave on to the CCD array. If the wave is planar, the light focused will hit the null space between CCD sensors, but if the wavefront is distorted, the light will be focused on the CCD sensor. By calculating the horizontal displacement of the light spot, the sensor reconstructs the wavefront distortion. For example, in Figure 2, the focused light is hitting the point Δy away from the reference point. In this case, when we let the distance between the sensor and the lens array be z , the slope of the incoming light ray is as follows.

$$\text{slope} = \frac{\Delta y}{z} \quad (6)$$

By repeating the calculation for each point on the screen, the sensor can reconstruct the wavefront of the light rays.

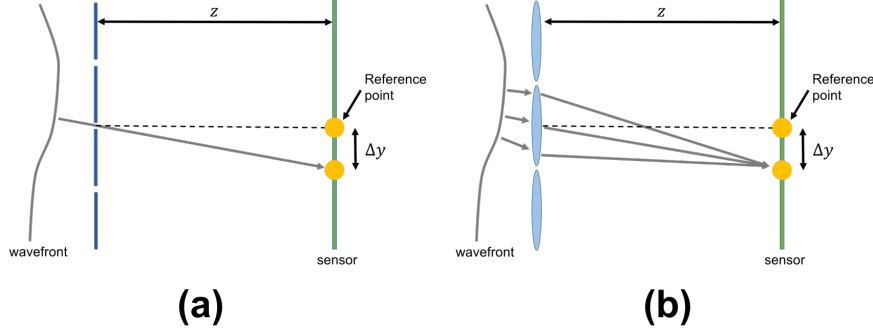


Fig. 2.— Shack-Hartmann sensor: The sensor uses an array of CCDs to detect the distortion of wavefront. When a wavefront hits the screen of lens, in which each lenslet is designed to focus the light to the reference points right between CCDs. However, if the wavefront is not planar, the rays do not hit the reference points. The sensor calculates the horizontal displacement of the point where the rays are focused from the reference point. (a) Original Hartmann screen (b) Shack improvement of the Hartmann test.

However, since the rays are not focused on a perfect point, the sensor uses a special procedure called a “quad cell technique,” which is a means of calculating the diversion of rays based on the intensity distribution over four adjacent cells. In Figure 3, the ray is slightly tilted to quadrant 1.

When I_1, I_2, I_3, I_4 are the intensity of the light measured at each cell, and b is the diameter of the light spot, the displacements from the reference point, which is the origin in the figure, can be estimated as follows.

$$\delta x = \frac{b}{2} \left[\frac{(I_1 + I_4) - (I_2 + I_3)}{I_1 + I_2 + I_3 + I_4} \right] \quad (7)$$

$$\delta y = \frac{b}{2} \left[\frac{(I_1 + I_2) - (I_3 + I_4)}{I_1 + I_2 + I_3 + I_4} \right] \quad (8)$$

As the sensor calculates the wavefront distortion, it sends the information to the deformable mirror to cancel out the noise.

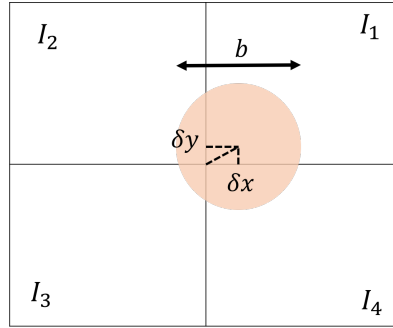


Fig. 3.— Quad Cell technique: The reference point is located at the center of the grid, and the light spot is tilted slightly to the upper-right direction. To calculate the displacement of the spot from the reference point, the sensor uses the intensity distribution over four cells.

2.3. Deformable mirror

Deformable mirrors are the adaptive components that counter the wavefront distortion and reduce the noise in the image. By deforming the surface of the mirror in a way that reflected wave will restore its original wavefront, the mirror corrects the image, and the wave goes to the beam splitter so that it forms an image on the screen and is processed by the wavefront sensor at the same time. There are several different types of deformable mirror. First is the segmented mirror.

A segmented mirror consists of several different segments of mirrors which can be controlled independently by actuators. Since most wavefront sensors measure distortion for certain subarea, segmented mirrors are easy to control. High degree of freedom achieved by a great number of actuators make it easy to control each segment separately. However, there are some drawbacks of this technology. Because the mirror is separated into segments, there exist gaps between segments and they cause loss of information, extra infrared thermal emission, and diffraction. Such loss is negligible in solar application, but for nighttime application, it causes a significant change.

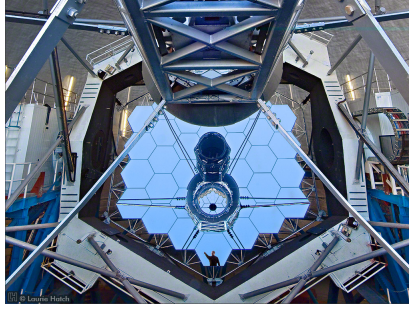


Fig. 4.— Primary mirror of the Keck II telescope: Telescopes of the Keck Observatory are equipped with adaptive optics technology. The figure is a primary mirror of Keck II telescope, one of the twin telescopes of the observatory. The mirror consists of several segments which can be controlled independently by actuators. Image Credit: Laurie Hatch Photography - <http://www.lauriehatch.com/>

Therefore, in conditions where segmented mirror is ineffective, continuous facesheet mirrors are regularly used.

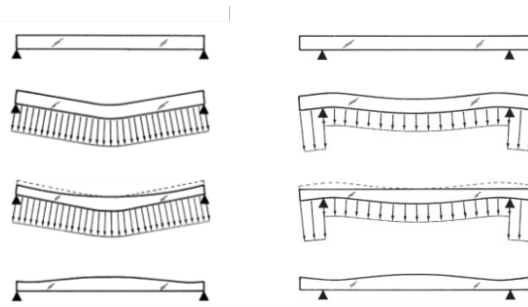


Fig. 5.— Deformation of continuous facesheet mirror: There are largely two methods of deforming a monolithic mirror. Figure on the left is a single-zone loading method, in which the moment is applied on single point, and the one on the right is a double-zone loading method, in which the moment is on two different points. Image Credit (Gerard R. Lemaitre 2013)

Continuous facesheet mirrors (CFS) deforms a monolithic mirror. It can be operated by reduced number of actuators as it is not controlling each component of the mirror, and the mirror retains its continuity by itself. The mirror used for the this type of deformation technique should be thick enough to maintain flatness during polishing and thin enough to be deformed by an actuator. Unlike segmented mirrors, continuous facesheet mirrors are naturally continuous, so they do not have problems related to gaps and loss of information (Jacque M. Beckers 1993).

There are some other types of deformable mirror technology, and the improvement of the technique is still continuing. Bimorph mirror is a type which deforms its surface by a bending moment created by transverse piezoelectric plates. The principle of the bimorph mirror is similar to that of a bimetal. Transverse plates made of piezoelectric ceramic materials form the surface

of the mirror, and the contraction of the plate to transverse direction causes a bending moment (Madec 2012). There have been some attempts of using electrodes instead of mechanical actuator, and it was proven that such method has advantages over conventional methods. (Wang et al. 2009) These methods are usually called as microelectromechanical systems (MEMS) technology. The surface of the MEMS deformable mirrors are controlled by electrostatic machining in a micro level. One of the biggest strengths of the technology is a spatial efficiency. The actuators of the MEMS can be integrated on a chip much smaller than the size of a mechanical actuators. There also is a method of using liquid crystal materials as an adaptive component. Voice coil mirror is a technology that uses an actuator powered by magnetic field. Voice Coil mirrors have some advantage in that it has less emissivity so that it is suitable for thermal infrared observation. However, it uses a very large actuators, so it costs a lot to build a large facility (Tyson 1998). Liquid crystal spatial light modulator (LC SLM) is a technology that uses liquid crystal materials to change the reflected wavefront (Bonaccini et al. 1992).

Table 1: Deformable mirror technology: Electrostrictive actuators are powered by electric field and piezoelectric actuators are powered by voltage across it. CFS: Continuous Facesheet Mirror, MEMS: Microelectromechanical System, LC SLM: Liquid Crystal Spatial Light Modulation

Type	Deformation mechanism	type
Stacked array	Electrostrictive/Piezoelectric	CFS/Segmented
Bimorph	Piezoelectric	CFS
MEMS	Electro/Magnetic	CFS/Segmented
Voice coil	Magnetic	CFS
LC SLM	Electro optic	LC SLM

3. Simulation

Considering the components of adaptive optics introduced above, distortion by atmosphere, wavefront sensor, and deformable mirror, we can simulate the process of the technology in a very simplified fashion.

The distortion of wavefront by an atmosphere is caused because each ray entering the atmosphere is passing through the “packet” of air with a different density and with a different refractive index. Based on the analysis of the Kolomogorov structure function, we could conclude that the refractive indices of the air differ only by certain amount from their adjacent points. Therefore, I modelled an atmosphere as an array of refractive index of number around unity. (i.e. $n \in [0.8, 1.2]$) Each entry of the array indicates a point on the air, so when a ray passes through the air, the ray experiences a refractive index of the entry corresponding to the position of the ray relative to the atmosphere.

Figure 6 shows the modeling of the atmosphere in a schematic way. Refractive index can be

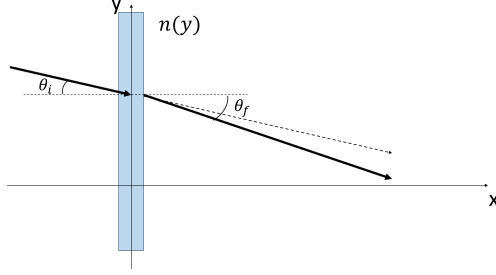


Fig. 6.— Atmospheric distortion of ray in two-dimensional case: The atmosphere has different values of refractive indices for different positions. When a ray passes through a certain point on the atmosphere, it experiences a value associated with the point and is refracted.

described as a function of relative position on the atmosphere, and we can use the simplified Snell's law to determine how much a ray is refracted. When θ_i is an angle of incidence and θ_f is an angle of refraction, the relationship between two can be described as follows.

$$\sin(\theta_i) = n(y) \sin(\theta_f) \quad (9)$$

In the three dimensional case, we can do the same analysis for two different planes to get the direction of the ray after passing through the atmosphere.

After the ray is distorted, it goes to the lens, which is a telescope in real situation. In a real adaptive optics technology, a wavefront sensor, a deformable mirror, and a telescope are separate entities, but in a simulation, a concept of "adaptive lens" is introduced to simplify the situation. An adaptive lens functions as both wavefront sensor and deformable mirror. When ray hits the lens, it measures the distortion by the atmosphere by measuring the horizontal distance from the reference point, and based on the calculation, it distorts the ray more than a simple lens would do.

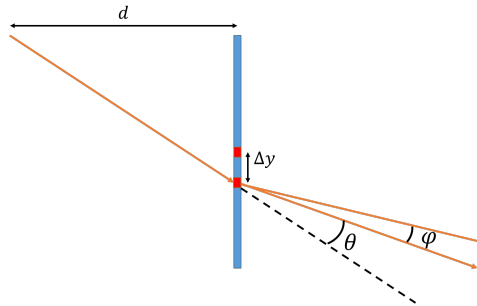


Fig. 7.— Modelling of an adaptive lens: When a ray hits the lens, a lens calculates the distortion of the ray by its displacement from the reference point. If θ is an angle that an ordinary lens would refract the ray, an adaptive lens will refract it more or less by a correction factor of ϕ .

Figure 7 describes the procedure. The calculation of the wavefront distortion follows the method introduced above, and based on the calculation, the lens calculates a correction factor ϕ .

When the focal length of the lens is f and the ray is coming from a point of which the horizontal distance from the lens is $2f$, the correction factor is calculated as follows.

$$\tan \phi = -\frac{\Delta y}{d} + \frac{\Delta y}{2f} \quad (10)$$

The first term cancels out the distortion by atmosphere, but there is one more thing that should be considered in this simulation. As the point where ray hits the lens is different because of the atmospheric distortion, the rays do not converge on one point. When an object is far from the telescope, the effect is negligible, but in the simulation, such correction is necessary.

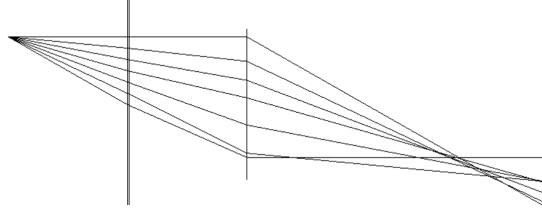


Fig. 8.— Modelling of an atmospheric distortion: The rays do not converge on one point.

Figure 8 is a two-dimensional simulation of an atmospheric distortion. As the ray meets an atmosphere and undergoes a refraction, the rays do not converge at one point after passing through the lens, and creates a blurred image. However, with an adaptive process, the result is different.

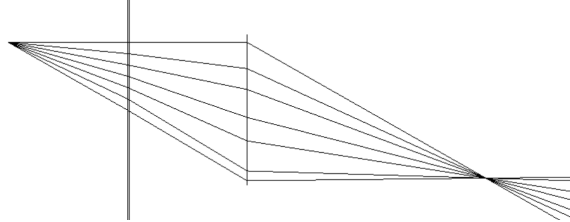


Fig. 9.— Correction of atmospheric distortion by adaptive process: The rays are refracted as it passes through the atmosphere, but they converge at one point because of the adaptive lens.

In Figure 9, although rays are tilted by the atmosphere, the lens detects the distortion in the wavefront and corrects it by refracting the rays more by a correction factor calculated above. As a result, the rays converge at one point, thereby creating a clean image.

Using the basic modelling introduced above, we can finally model the distortion of image by an atmosphere and its correction. The basic concept is similar, but to model the image, we need a three-dimensional approach to both wavefront sensor and adaptive lens. We can model an atmosphere as a two-dimensional array and calculate the correction factor using a derivative of the ray's direction. Therefore, Equation 9 and Equation 10 change as follows.

$$(\theta_{x,i}, \theta_{y,i}) = (n(x, y)\theta_{x,f}, n(x, y)\theta_{y,f}) \quad (11)$$

$$(\tan \phi_x, \tan \phi_y) = \left(-\frac{\Delta x}{d} + \frac{\Delta x}{2f}, -\frac{\Delta y}{d} + \frac{\Delta y}{2f} \right) \quad (12)$$

A subscript x and y under θ and ϕ means that they are an angle that the projection of a vector, the direction of the ray, to a x-z plane and y-z plane forms with z axis. Therefore, it is much easier to work with derivatives, $\frac{\partial x}{\partial z}$ and $\frac{\partial y}{\partial z}$, rather than angles. Figure 10 describes the process of the simulation.

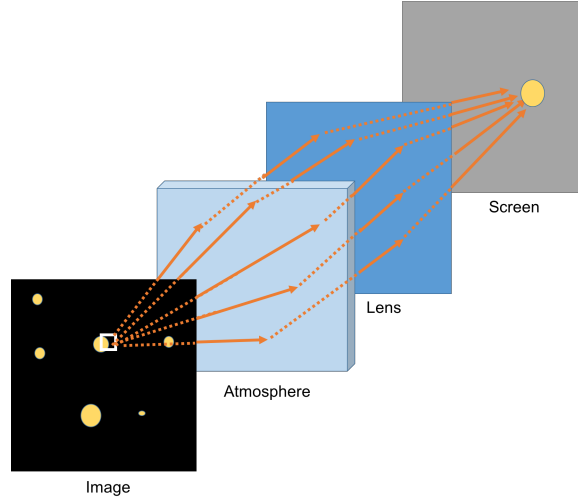


Fig. 10.— Schematic of the simulation: The simulation is based on the ray tracing method. The rays carrying the color information of certain point of the image goes to several directions, and distorted by the atmosphere. The rays are then refracted by the lens and hit the screen that is away from the lens a certain distance. When the ray hits the screen, the ray stores the information it was carrying to the screen. The process is repeated for all the points of the image pixel by pixel.

The atmosphere in the simulation is modeled as a 2d-array of random refractive index in the range of $[0.9, 1.1]$. It does not satisfy the Kolmogorov turbulence model, but it fulfills its purpose of distorting the incoming wavefront. 11 shows the atmosphere used in the simulation.

Figure 13 is the result of the simulation on the image of Pleiades star cluster. The image distorted by the atmospheric distortion is darker and blurry, as the rays from the original image are not concentrated on one point. The image fixed by an adaptive process is almost perfectly reconstructed, but this is not possible in real observations. First, in my simulation, the adaptive process took place for each incoming ray consecutively. This procedure is slightly different from real situation, because all the right rays hit the deformable mirror at the same time, not one at a time. Second, the simulation is devoid of mechanical errors which take place in the telescope, such as additional thermal radiation and loss of information due to gap between mirror segments.

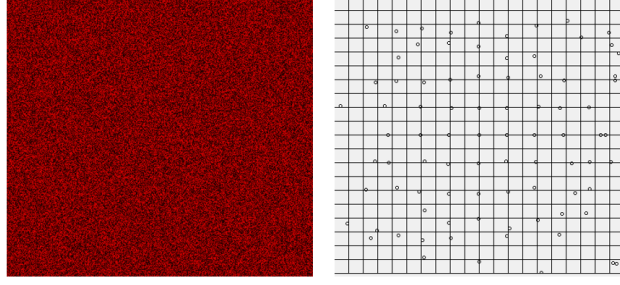


Fig. 11.— Atmosphere and wavefront sensor used in simulation: Figure on the left represents the atmosphere with randomly selected refractive indices. Figure on the right shows a wavefront sensor used in the simulation. Small circles indicate places on which light rays hit, and they are away from the sensor's grid points, which are the reference points.

Although adaptive optics does not give a perfect reconstruction of image like the simulation, it is a groundbreaking technology that enabled a large improvement of the high-precision observation.



Fig. 12.— Simulation of image distortion by atmosphere and the correction by adaptive process: An image on the left has a darker and more blurry image, while the image fixed by adaptive process is much more accurate. Original Image is adapted from Astronomy Picture of the Day 2007 Nov. 18th

REFERENCES

- Jacque M. Beckers, 1993, Adaptive Optics For Astronomy: Principles, Performance, and Application, *Annu. Rev. Astron. Astrophys.* 1993.31:13 - 62
- Babcock, H. W. 1953, The Possibility of Compensating Astronomical Seeing *PASP*, 65, 229

- Gerard R. Lemaitre, Optical Design and Active Optics Methods in Astronomy, Optical Review Vol. 20, No. 2 (2013) 103 - 117
- N. J. Woolf, High Resolution Imaging From The Ground, Annu. Rev. Astron. Astrophys. 1982.20:367 - 98
- Hartmann, J. 1900, Remarks on the Construction and Adjustment of Spectrographs. ApJ, 11, 400
- Merkle, F. 1986, Adaptive Optics for the VLT. European Southern Observatory Conference and Workshop Proceedings, 24, 443
- Bonaccini, D., Brusa, G., Esposito, S., et al. 1992, Adaptive optics wavefront corrector using addressable liquid-crystal retarders: II, Proc. SPIE, 1543, 133
- Wang, D. J., Yao, J., Qiu, C. K., Hu, F. R., & Fan, T. Q. 2009, Journal of Vacuum Science Technology B: Microelectronics and Nanometer Structures, 27, 1291
- Tyson, R. K. 1998, Principles of adaptive optics, Edition: 2nd ed., Publisher: Boston, MA: Academic Press, 1998, ISBN: 0127059024,
- Duffner, Robert W, The adaptive optics revolution : a history (2009)
- Madec, P.-Y. 2012, Proc. SPIE, 8447, 844705 Overview of Deformable Mirror Technologies for Adaptive Optics and Astronomy

Appendix

A. Class Diagram of the Simulation Program

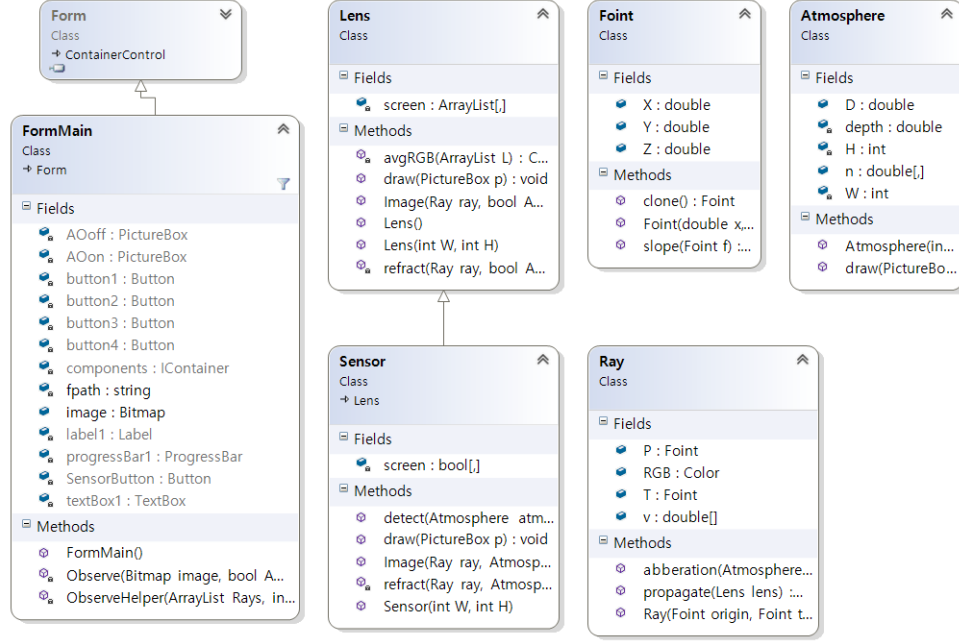


Fig. 13.— Class diagram of the computer program on which the simulation runs: Class Ray is an object which is used for the ray tracing. Each Ray object contains a color information of the original image. Class Lens is an adaptive component which refracts rays to form an image. Class Sensor inherits the class Lens, but its major functionality is to detect wavefront distortion. Class Atmosphere contains a 2D-array of refractive indices. Class Foint represents a three dimensional coordinate. Using above classes, the main form calls an Observe method to simulate a process of adaptive Optics.

B. Source of the Simulation

B.1. Class: Ray

```
public class Ray
{
    public Foint T;
    public double[] v;
    public Foint P;
    public Color RGB;

    public Ray(Foint origin, Foint target, Color c)
    {
        T = target;
        v = origin.slope(target);
        P = origin.clone();
        RGB = c;
    }

    public void propagate(Lens lens)
    {
        double d = - this.P.Z;
        this.P.X += this.v[0] * d;
        this.P.Y += this.v[1] * d;
        this.P.Z = 0;
    }

    public void abberation(Atmosphere atm)
    {
        double D = atm.D;
        this.P.Z += D;
        this.P.X += this.v[0] * D;
        this.P.Y += this.v[1] * D;
        int x = (int)(this.P.X + atm.n.GetLength(0)/2);
        int y = (int)(this.P.Y + atm.n.GetLength(1)/2);
        this.v[0] = Math.Tan(Math.Asin(Math.Sin(Math.Atan(v[0])) / atm.n[x, y]));
        this.v[1] = Math.Tan(Math.Asin(Math.Sin(Math.Atan(v[1])) / atm.n[x, y]));
    }
}
```

B.2. Class: Atmosphere

```
public class Atmosphere
{
    public double D;
    public double[,] n;
    private int W;
    private int H;
    private double depth = 0.1;

    public Atmosphere(int w, int h, int d)
    {
        W = w;
        H = h;
        D = d;
        n = new double[w, h];
        Random orand = new Random();
        for (int x = 0; x < w; x++)
        {
            for (int y = 0; y < h; y++)
            {
                n[x, y] = 1 + orand.NextDouble() * 2 * depth - depth;
            }
        }
    }
}
```

B.3. Class: Foint

```
public class Foint
{
    public double X = 0;
    public double Y = 0;
    public double Z = 0;

    public Foint(double x, double y, double z)
    {
        X = x;
        Y = y;
        Z = z;
    }

    public double[] slope(Foint f)
    {
        double[] v = new double[2];
        v[0] = (double)(X - f.X)/(Z - f.Z);
        v[1] = (double)(Y - f.Y)/(Z - f.Z);
    }
}
```



```

        return v;
    }
}

```

B.4. Class: Lens

```

public class Lens
{
    ArrayList[,] screen;

    public Lens()
    {

    }

    public Lens(int W, int H)
    {
        screen = new ArrayList[W, H];
        for (int x = 0; x < W; x++)
        {
            for (int y = 0; y < H; y++)
            {
                screen[x, y] = new ArrayList();
            }
        }
    }

    public void Image(Ray ray, bool AO, Atmosphere atm){
        refract(ray, AO, atm);
        ray.P.X += ray.v[0] * 100 + screen.GetLength(0)/2;
        ray.P.Y += ray.v[1] * 100 + screen.GetLength(1)/2;
        ray.P.Z = 100;
        int x = (int)ray.P.X;
        int y = (int)ray.P.Y;
        if (x < screen.GetLength(0) && y < screen.GetLength(1) && x > 0 && y > 0)
        {
            screen[x, y].Add(ray.RGB);
        }
    }

    private void refract(Ray ray, bool AO, Atmosphere atm)
    {
        if (AO)
        {
            double d = 100 - atm.D;
            double CFx = (ray.P.X - ray.T.X) * (-1.0 / d + 1.0 / 100.0);

```

```

        double CFy = (ray.P.Y - ray.T.Y) * (-1.0 / d + 1.0 / 100.0);
        ray.v[0] = -(double)ray.P.X / 50 + ray.v[0] + CFx;
        ray.v[1] = -(double)ray.P.Y / 50 + ray.v[1] + CFy;
    }
    else
    {
        ray.v[0] = -(double)ray.P.X / 50 + ray.v[0];
        ray.v[1] = -(double)ray.P.Y / 50 + ray.v[1];
    }
}

public void draw(PictureBox p)
{
    p.Image = new Bitmap(screen.GetLength(0), screen.GetLength(1));

    for (int x = 0; x < screen.GetLength(0); x++)
    {
        for (int y = 0; y < screen.GetLength(1); y++)
        {
            ((Bitmap)p.Image).SetPixel(x, screen.GetLength(1) - 1 - y, avgRGB(screen[x
        ]
    }
    p.Refresh();
}

private Color avgRGB(ArrayList L)
{
    int R = 0;
    int G = 0;
    int B = 0;
    int total = 0;
    foreach (Color c in L)
    {
        R += c.R;
        G += c.G;
        B += c.B;
        total++;
    }
    if (total < 4)
    {
        return Color.FromArgb(0, 0, 0);
    }
    else
    {
        return Color.FromArgb(R / total, G / total, B / total);
    }
}

```

```

    }
}

```

B.5. Method: Observe

```

private void Observe(Bitmap image, bool AO, PictureBox p)
{
    ArrayList Rays = new ArrayList();
    int W = image.Width;
    int H = image.Height;
    Lens lens = new Lens(W, H);
    Atmosphere atm = new Atmosphere(W, H, 50);
    progressBar1.Value = 0;
    progressBar1.Maximum = W * H;
    for (int x = 0; x < W; x++)
    {
        for (int y = 0; y < H; y++)
        {
            Color c = image.GetPixel(x,y);
            if (c.R > 10 || c.G > 10 || c.B > 10)
            {
                ObserveHelper(Rays, W, H, image, x, y);
                foreach (Ray ray in Rays)
                {
                    ray.abberation(atm);
                    ray.propagate(lens);
                    lens.Image(ray, AO, atm);
                }
                Rays.Clear();
            }
            progressBar1.Value++;
        }
    }
    lens.draw(p);
}

private void ObserveHelper(ArrayList Rays, int W, int H, Bitmap image, int x0, int y0)
{
    for (int x = W/5; x < W; x+= W/5)
    {
        for (int y = H/5; y < H; y+= H/5)
        {
            int xo = x0 - W / 2;
            int yo = y0 - H / 2;
            Rays.Add(new Ray(new Foint(xo,yo,-100), new Foint(x - W/2, y - H/2,0), image.G

```

}
}
}